Presentation of Novel High Torque Density Dual-Stator Wound-Field Flux Modulation Machines

U. B. Akuru and M. J. Kamper

***Abstract* – An attempt is made in this paper to present some novel wound-field flux modulating machines (WF-FMMs) based on the double stator (DS) design topology. The idea is to utilise the large split ratios eminent in WF-FFMs to boost the torque density and provide potential as alternative non-PM machines for direct-drive systems. The study involves the electromagnetic finite element analysis of four different DS WF-FFMs conceived by combining the outer and inner stator design of the wound-field flux switching machine and DC-excited Vernier reluctance machine. In the end, the objective of obtaining distinct DS machines with propensity for high torque density, low torque ripple and high efficiency is achieved, with a promise of future works in terms of machine optimisation and experimentation.**

***Index Terms*—DC Vernier reluctance machine (DC-VRM), double stator (DS), finite element analyses (FEA), torque, wound-field flux modulating machine (WF-FMM), wound-field flux switching machine (WF-FSM).**

I. Introduction

OVER the years, conventional (rotor-based) permanent magnet (PM) machines are preferred in applications such as in electric vehicles and wind power generators, given their high torque density, efficiency and robust rotor. But in recent times, PMs have become vulnerable due to fluctuating pricing and market monopoly of the relevant high-energy rare-earth resource, coupled with their demagnetisation susceptibility and thermal management issues [1]. To this end, there is a rat race towards finding a competitive alternative. The existence of the conventional electrically-excited machines is noted, but they have not produced respite because, apart from their low torque density and efficiency, they have low reliability.

To this end, there are novel and emerging electrical machine technologies which can be designed as non–PM (electrically-excited) machines. These machine variants are distinguished from their conventional counterparts in that they completely eliminate the need for brushes and slip rings in their DC windings set-up, while exhibiting the very same robust rotor topology of conventional PM machines. These are broadly called wound-field flux modulation machines (WF-FMMs), operating mainly under the principle of flux modulation, due to characteristic magnetic gearing effects [2], [3]. Examples of these emerging and promising class of stator-mounted brushless (commutator-less) machines are the so-called DC field-excited double salient machines (DC-DSMs), DC field-excited flux reversal machines (DC-FRMs), wound-field flux switching machines (WF-FSMs) and DC-excited Vernier reluctance machines (DC-VRMs) [4]–[7], among others. However, because of the absence of PMs, and the fact that these machines exhibit higher split ratios, their torque density and efficiency can decline [8].

Hence, to exploit the large space etched inside the inner rotor, and occasioned by high split ratios, the dual-stator (DS) machine topology is being proposed in this study. DS machines have advantages ranging from high flexibility and fault-tolerant capability, to exhibiting compact structure and high torque density, which maximises volume and improves utilisation index between materials and space [9]-[11].

In the past, attempts have been made towards designing DS FMMs such as the WF-FSM with double stators. Based on what is prevalent, i.e., the so-called partition-stator (PS) machines, the torque density is not improved as much as in a topology supporting the electromagnetic duplication of the inner and outer stators [12], [13]. However, in PS-WF machines, slight improvement on efficiency can be envisaged since the armature and field windings are separately accommodated in the outer and inner stators, respectively [11].

Although, DS PM-FSMs with duplicated stators have been designed and evaluated as well [10], the same cannot be said of WF-FSMs or any other WF-FMM. In the least, a DC-biased double-stator hybrid flux switching permanent-magnet machine is proposed and analysed in [14], but the proposed design is fraught with a complex drive system, and the need for PM utilisation in the design architecture. To this end, the performance characterisation of a DS WF-FMM remains to be seen, especially given the promising candidature posed by a duplicated stator topology for fault-tolerant rare-earth-free high-torque density direct-drive applications. Furthermore, such a design will promote field regulation of excitation system for flux weakening or enhancement performance. With the double stator housing all active components, a brushless operation and a simplistic thermal infrastructure can also be facilitated.

Therefore, in this paper, four DS WF-FMMs are proposed and implemented based on different combinations of the single-stator WF-FSM and DC-VRM topologies. The four distinct novel designs as envisaged are presented in the following section, and are based on some selected design specifications. In section III, electromagnetic modelling and performance analysis are carried out in 2D finite element analysis (FEA) and coupled circuit analysis. Section IV provides briefing on the performance evaluation with emphasis on the flux linkage,

This work is based on the research supported in part by the National Research Foundation of South Africa (Grant Number 127391).

U. B. Akuru is with Department of Electrical Engineering, Tshwane University, Pretoria Campus, 0183, South Africa. He is also affiliated to the Department of Electrical and Electronic Engineering, Stellenbosch University, Stellenbosch, Cape Town, 7600, South Africa and the Department of Electrical Engineering, University of Nigeria, Nsukka, 410001, Nigeria (e-mail: AkuruUB@tut.ac.za).

M. J. Kamper is with Department of Electrical and Electronic Engineering, Stellenbosch University, Stellenbosch, Cape Town, 7600, South Africa (e-mail: kamper@sun.ac.za).

978-1-7281-9944-3/20/$31.00 ©2020 IEEE

electromagnetic torque, cogging torque/torque ripple, power factor, efficiency, flux regulation and overload capability. The last section is used to draw some important conclusions.

II. Topology Formation and Presentation

The three-phase 24-stator slots/10-rotor poles (24/10) WF-FSM originates from the 12/10 PM-FSM, and has been widely analysed for performance and various application needs. Among other things, its popularity is built on simplistic design, fairly good winding factor and balanced symmetrical back-EMF waveforms [15]. On the other hand, the DC-VRM design is a more recent concept, of which the three-phase 12/10 topology is intrinsic but can exhibit asymmetric flux linkage and back-EMF under heavy load [3], [16]. It is equally reported that due to the torque/copper loss ratio, a higher stator slot number topology as the 12/10 design is more suitable for large-scale machines, suggesting a relevance for high torque density direct-drive applications [17]. To this end, the 24/10 WF-FSM and the 12/10 DC-VRM are primed for this study. This is based on the fact that they both possess robust rotor structures and balanced magnetic forces, as well as a designation for non-overlapping concentrated windings which translates to shorter end-windings and improved efficiency. In terms of their operating principles, a good account has been given in [3], [18], [19], based on flux modulation principles.

The design concepts of the WF-FSM and DC-VRM machines as investigated in this study are presented in Fig. 1, with the outer stator (OS) and inner stator (IS) concepts indicated. Four combinations to create the novel DS designs are evolved and christened as follows: WF-FMM1—combined WF-FSM inner and outer stators (*DS1*), WF-FMM2—combined DC-VRM inner and outer stators (*DS2*), WF-FMM3—combined WF-FSM inner and DC-VRM outer stators (*DS3*), and WF-FMM4—combined DC-VRM inner and WF-FSM outer stator (*DS4*).

Table I gives the main dimensions from which the conceptual DS WF-FMM designs are based. It is clear that similar current densities (J_f and J_s), as well as split ratios have been preserved in the study to ensure some comparative fairness. Besides, it can also be seen that larger split ratio (D_i/D_o) evolve in the single-stator variants of these machines, which is being capitalised in the proposed DS machines to improve their torque density. In Table I, D_{gos} and D_{gis} are indicative of the outer and inner stator airgap diameters, respectively.

It should be noted that, from the parameters given in Table I, all the studied machines have not been optimised. The modelling and performance evaluation of these machines in 2D FEA are discussed in the next section.

III. FEA Modelling and Electromagnetic Evaluation

The proposed modelling is done using an in-house 2D FEA time-stepped magnetostatic package called SEMFEM [20]. Analysis in SEMFEM is done based on Python script coding which allows for analytical modelling of the steady-state d- and q-axes flux linkages in rotor reference frame after supplying the necessary input current densities. In generator modes, the dq flux linkages are given as

$$\lambda_d = -L_d I_d + L_f I_f \quad (1)$$

$$\lambda_q = -L_q I_q, \quad (2)$$

where L_d and L_q are the dq inductances, I_d and I_q are the dq currents, L_f is the field-winding inductance and I_f is the DC field current. To simplify the modelling, a non-existent magnetic coupling between the q-axis and the field is assumed, otherwise this is usually not true in WF-FMMs [21].

Thus, the WF-FFM (both for single and double-stator) steady-state dq voltage equations are given as:

$$V_d = -R_s I_d - \omega_e \lambda_q + \omega_e L_e I_q \quad (3)$$

$$V_q = -R_s I_q + \omega_e \lambda_d - \omega_e L_e I_d, \quad (4)$$

where R_s is total phase-winding resistance with end-winding effects, ω_e is electrical speed and L_e is end-inductance.

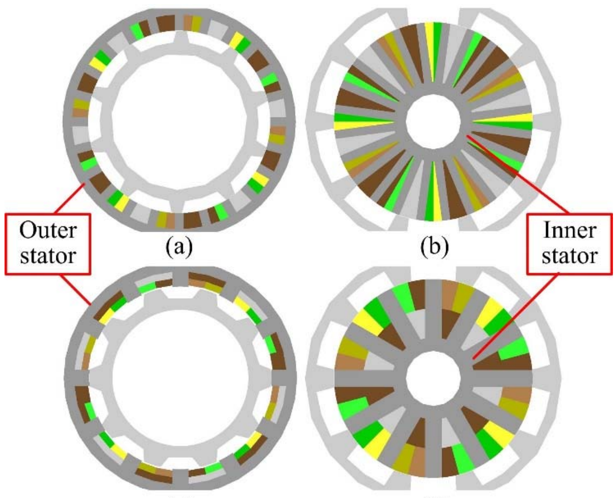

Fig. 1. Considered WF-FMM topologies: (a) OS-WF-FSM, (b) IS-WF-FSM, (c) OS-DC-VRM, and (d) IS-DC-VRM.

TABLE I
Design Parameters

	J_s A/mm²	J_f A/mm²	k_s -	k_f -	Ω_m r/min	l/D_i -	D_i/D_o -	g mm	D_o mm	D_i mm	l mm	D_{gos} mm	D_{gis} mm
OS-WF-FSM	3.5	4.2	0.45	0.45	300	0.16	0.78	0.8	1200	937.5	150	-	-
IS-WF-FSM	3.5	4.2	0.45	0.45	300	0.28	0.78	0.8	700	542.8	150	-	-
OS-DC-VRM	3.5	4.2	0.45	0.45	300	0.16	0.78	0.8	1200	937.5	150	-	-
IS-DC-VRM	3.5	4.2	0.45	0.45	300	0.28	0.78	0.8	700	542.8	150	-	-
DS1	3.5	4.2	0.45	0.45	300	-	-	0.8	1200	-	150	936.7	542.0
DS2	3.5	4.2	0.45	0.45	300	-	-	0.8	1200	-	150	936.7	542.0
DS3	3.5	4.2	0.45	0.45	300	-	-	0.8	1200	-	150	936.7	542.0
DS4	3.5	4.2	0.45	0.45	300	-	-	0.8	1200	-	150	936.7	542.0

N.B. J_s and J_f = armature and field current densities, k_s and k_f = armature and field winding slot fill factors, l = stack length, D_i = stator inner diameter, D_o = stator outer diameter, g = airgap length, D_{gos} = stator airgap outer diameter, D_{gis} = stator airgap inner diameter

With $I_d = 0$ current control and $R_s = 0$ for simplicity, a sample WF-FSM space phasor diagram is as shown in Fig. 2, with δ being the power angle. The true power, reactive power and power factor are then calculated as

$$P = \frac{3}{2}\left(V_d I_d + V_q I_q\right) \tag{5}$$

$$Q = \frac{3}{2}\left(V_d I_q - V_q I_d\right) \tag{6}$$

$$S = \sqrt{P^2 + Q^2} \tag{7}$$

$$PF = \cos\phi = \frac{P}{S}. \tag{8}$$

The electromagnetic torque, considering the generator power flow model, is calculated as

$$\tau_e = \frac{3}{2} N_r \left(\lambda_d I_q - \lambda_q I_d\right), \tag{9}$$

where N_r the number of rotor teeth.

Notwithstanding, the distinct core loss, usually made up of the eddy current and hysteresis losses, is evaluated from the condensed Steinmetz's expression as follows:

$$P_{Fe} = c f_k^x \left(B_{tooth}^y M_{tooth} + B_{yoke}^y M_{yoke}\right), \tag{10}$$

where B_{tooth} and B_{yoke} are the maximum flux densities in the respective teeth and yoke of the stator and rotor cores, while M_{tooth} and M_{yoke} are the respective teeth and yoke mass of the stator and rotor. The variables c, x and y are the Steinmetz coefficients, which depend on the manufacturer's frequency-dependent loss characteristics of the core material. The frequency, f_k, depends on the stator, 's' and rotor, 'r' components in WF-FMMs, defined respectively for a single-rotor single-stator machine as [22]:

$$f_s = \frac{N_r \Omega_m}{60} \tag{11}$$

$$f_r = \frac{N_s \Omega_m}{120}, \tag{12}$$

where Ω_m is the rotor speed and N_s, the number of stator slots. But for the proposed DS WF-FMMs, f_r is redefined as

$$f_r = \frac{f_s}{4}. \tag{13}$$

The phase and field winding copper losses are then given as

$$P_{cus} = \frac{3}{2} R_s \left(I_d^2 + I_q^2\right), \tag{14}$$

$$P_{cuf} = I_f^2 R_f, \tag{15}$$

where I_f and R_f are the field winding current and total resistance, respectively.

The machine efficiency, without taking into account the wind-and-friction losses, is given as

$$\eta = \frac{P}{P + P_{Fe} + P_{cus} + P_{cuf}} \times 100\%. \tag{16}$$

IV. Performance Evaluation

The results presented in this section is, as earlier indicated, based on 2D time-stepping magneto-static FEA. In general, the conventional WF-FMMs shown in Fig. 1 are combined to yield the newly formed DS machines as shown in Fig. 3.

A. No-Load Performance

The no-load airgap flux densities in the proposed DS WF-FMMs are shown in Fig. 4. It can be seen that they are summed by their individual outer and inner stator airgap components. Although the plots in Fig. 4 are non-sinusoidal, a peak value of above 3.5 T is observed in all the machines, an indication of high torque density performance and magnetic saturation.

Plots of the no-load flux density and flux distribution are compared in Figs. 5–6. Because the machines are currently not optimised, very high core saturation and flux leakages are clearly observed even when $I_q = 0$. However, what is clear from these figures, especially Fig. 6, is the fact that the newly proposed DS WF-FMMs exhibit balanced magnetic fields.

In Fig. 7, the cogging torque profiles are presented. Once again, the sum of individual values calculated in the outer and inner stator airgap components, yields the effective cogging torque of the DS designs. Although it is not clear from Fig. 7, but as later indicated in Table II, the cogging torque values greatly improved in the DS-WFFMMs compared to averaging the effects of the individual single-stator WF-FSM and DC-VRM. This, of course, is due to higher flux density in the DS designs as shown in Fig. 6 compared to Fig 5. [2].

The no-load dq flux linkages are plotted as shown in Figs. 8-9. As expected, the q-axis component is approximately zero since $I_q = 0$, while the average values of the newly proposed DS designs in Fig. 9 are gotten from approximately summing up the two respective single-stator designs in Fig. 8. Overall, the flux linkages under no-load clearly show the proper alignment of the initial rotor position to the d-axis. Also, the summative effects in λ_d are seen in Figs. 8-9, directly from FEA.

B. On-Load Performance and Other Characteristics

Fig. 10 shows the electromagnetic torque profiles of the newly proposed DS WF-FMMs at rated field and armature currents. From Table II, it is clearly seen that τ_e, for the DS machines, is the sum of its outer (τ_{eos}) and inner (τ_{eis}) stator components. It is also seen that the torque densities (τ_e/V_a) of the DS machines have been improved compared to their respective outer stator machines, by as much as 23.1 %, 22.7 %, 26.8 % and 20.7 % for *DS1*, *DS2*, *DS3* and *DS4*, respectively.

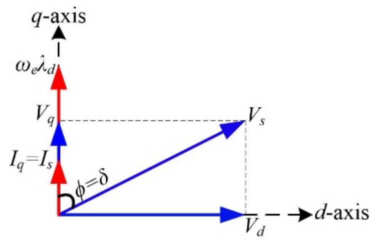

Fig. 2. WF-FMM phasor diagram in generating mode.

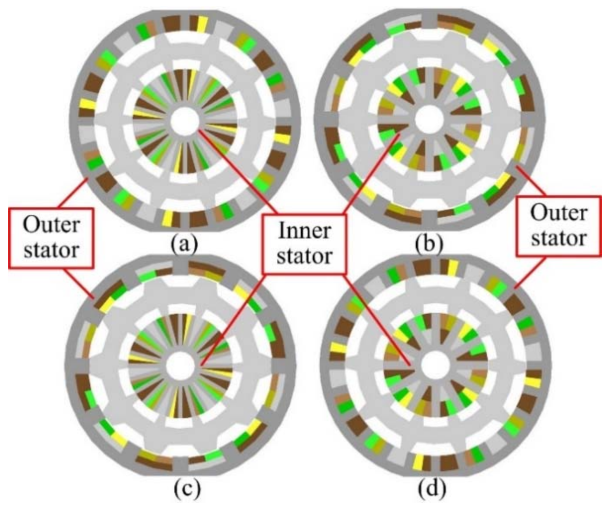

Fig. 3. Conceived DS WF-FMMs: (a) *DS1*, (b) *DS2*, (c) *DS3*, and *DS4*.

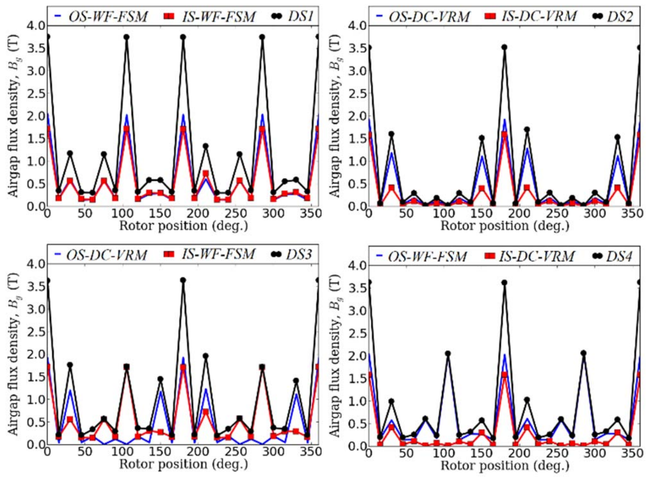

Fig. 4. Mid-airgap flux density analysis in the proposed DS WF-FMMs, showing both the outer and inner stator airgap components.

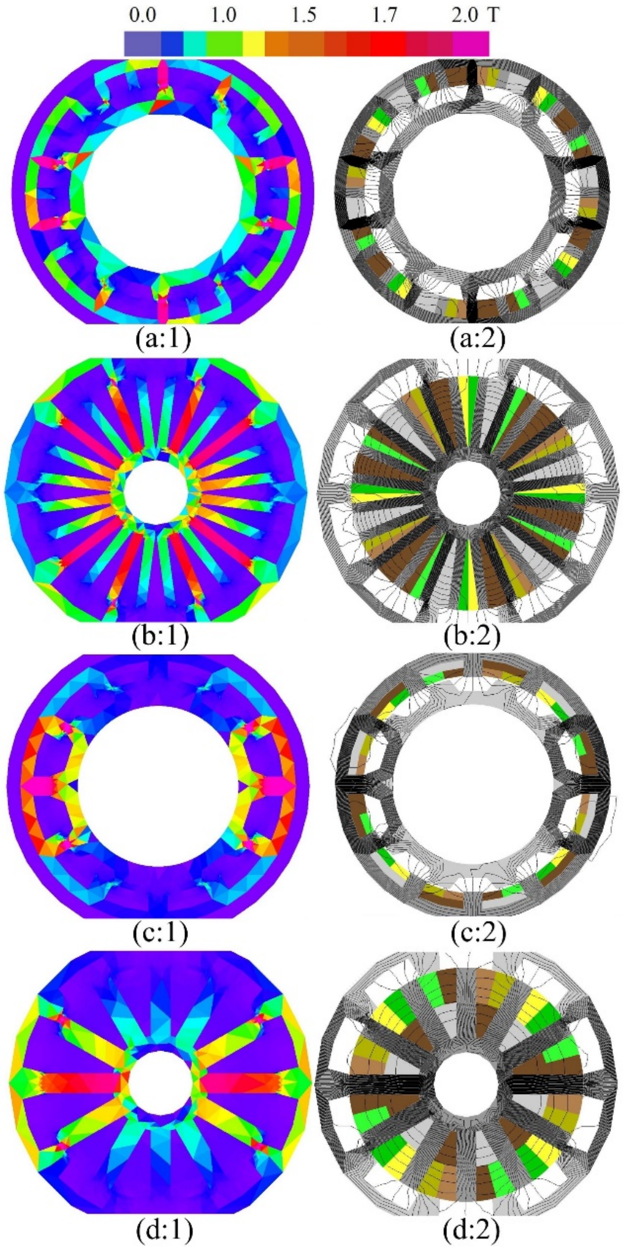

Fig. 5. No-load flux density map (1) and flux distribution lines (2): (a) OS-WF-FSM, (b) IS-WF-FSM, (c) OS-DC-VRM, and (d) IS-DC-VRM.

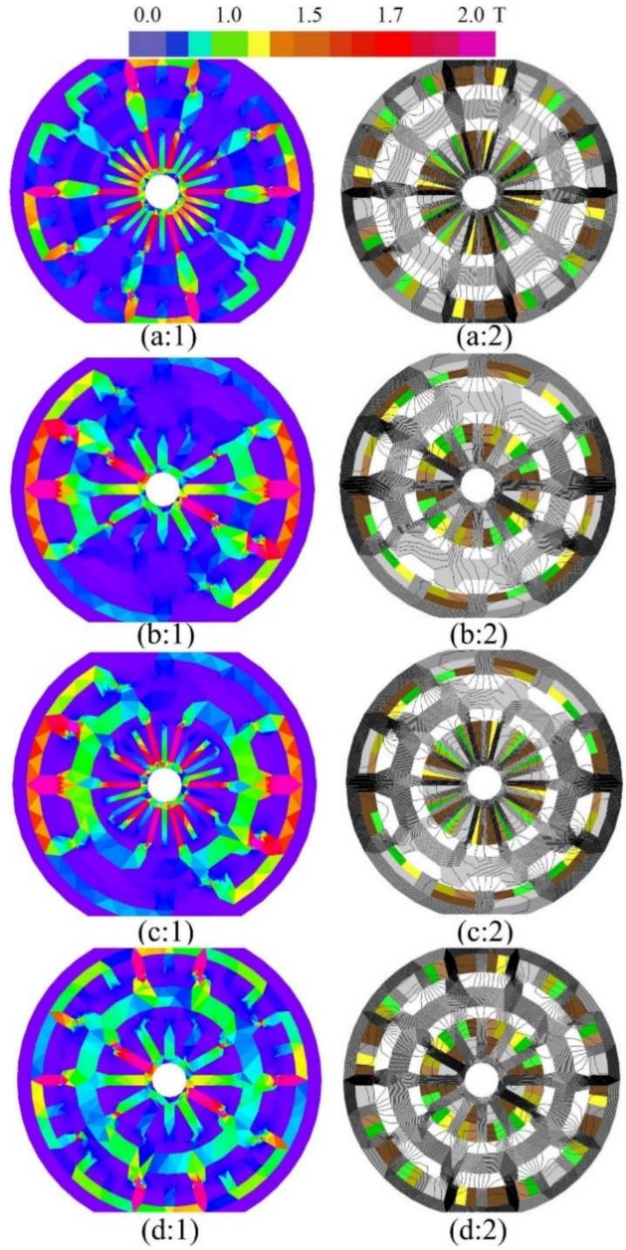

Fig. 6. No-load flux density map (1) and flux distribution lines (2): (a) *DS1*, (b) *DS2*, (c) *DS3*, and *DS4*.

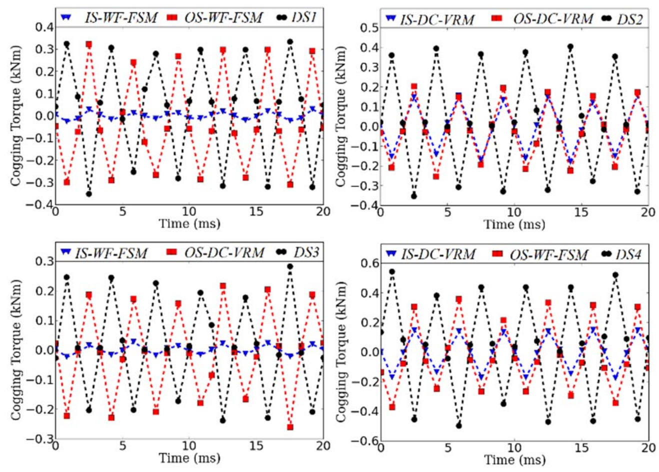

Fig. 7. Cogging torque analysis in the proposed DS WF-FMMs, showing both the outer and inner stator airgap components. λ_d

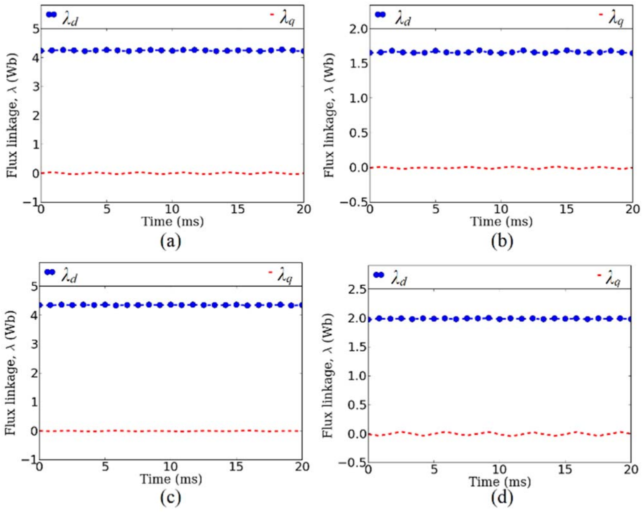

Fig. 8. No-load flux linkages in conventional WF-FMMs: (a) OS-WF-FSM, (b) IS-WF-FSM, (c) OS-DC-VRM, and (d) IS-DC-VRM.

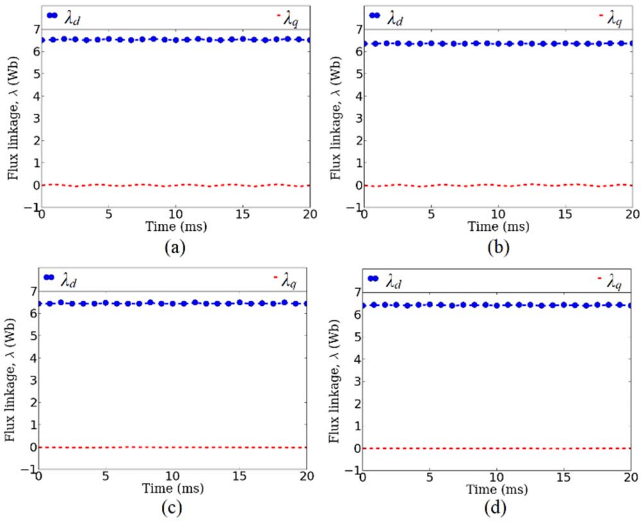

Fig. 9. No-load flux linkages in proposed DS WF-FMMs: (a) *DS1*, (b) *DS2*, (c) *DS3*, and *DS4*.

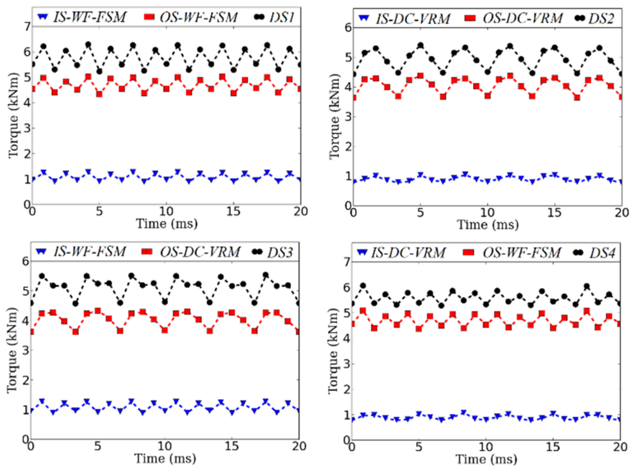

Fig. 10. Electromagnetic torque of the proposed DS WF-FMMs, showing both the outer and inner stator airgap components at rated conditions.

In terms of the torque ripple, major improvements are observed in the DS machines compared to the average values of the single-stator WF-FMMs, e.g., as much as 19.8 %, 19.8 %, 32.4 % and 32.9 % for *DS1*, *DS2*, *DS3* and *DS4*, respectively. Among other things, this can be attributed to torque ripple offsets observed in the single-stator inner and outer machines, especially in cases where DC-VRM and WF-FSM are combined to form the proposed DS machines (*DS3* and *DS4*). For instance, it is clearly seen that the component torque waveforms for *DS3* and *DS4* in Fig. 10 are not synchronised, a characteristics which is clearly not exhibited in the cogging torque of the proposed DS machines, as their waveforms of their single-stator machines are seen to be in phase. Again, it has to be said that the presented DS machines have not been optimised, for which we envisage improvements in the cogging torque and torque ripple quality after robust optimisation [23]. Our future studies will detail these results.

In terms of efficiency, the proposed DS WF-FMMs also yield good performance predictions as shown in Table II, with all the computations in excess of 93 %. This is a reliable operating margin based on the prescribed power ratings [24], and considering that the winding resistance is predicted at an operating temperature of 100 ºC. As a matter of fact, the efficiency improved when compared against the average of the single machines by up to 2.9 %, 3.3 %, 2.5 % and 3.2 % for *DS1*, *DS2*, *DS3* and *DS4*, respectively. Among others, a competitive efficiency performance for the DS machines should be expected since, as indicated in (13), the rotor core losses can reduce by up to 15 % compared to that of the convention.

Furthermore, Table II shows the total loss per active volume (P_L/V_a) mostly deteriorate for the DS WF-FFMs, albeit slightly. For example, compared to the average between the respective OS-DC-VRM and IS-DC-VRM combined effects, it increased by 46.8 %, 47.4 %, 42.3 % and 53.1 % for *DS1*, *DS2*, *DS3* and *DS4*, respectively.

The power factor computation for the proposed DS machines does not portray significant improvement compared to the single-stator machines. This is due to the fact that, ordinarily, WF-FMMs exhibit poor power factor because of their high flux leakage characteristics [19], which is exacerbated even for the proposed DS designs. The average values recorded for the DS machines in Table III are, to say the least, very realistic, but can be further improved by design optimisation.

In Figs. 11 and 12, overload capability and flux regulation analysis are undertaken for the studied WF-FMMs. Due to high magnetic saturation and flux leakages, it is seen that at rated field and armature currents, the torque peaks at 2 p.u. for majority of the proposed DS machines. This is not bad, granted that some PM-FMMs achieve peak points at less than 2 p.u. [25]. As shown in Fig.12, the overload capability can be easily improved by field enhancing or weakening, a proviso not guaranteed in PM machines. One can also observe that the back-EMF can be increased by weakening the field (reducing the field current) and decreased by enhancing the field (increasing the field current). It is seen that the rate of field enhancement is higher compared to field weakening due to dominating armature reaction effects.

TABLE II
EVALUATED PERFORMANCE DATA

	$\Delta\tau_{NL}$ %	$\Delta\tau_L$ %	P_{cuf} kW	P_{cus} kW	P_{Fes} kW	P_{Fer} kW	P_{Fe} kW	P_g kW	τ_{eos} kNm	τ_{eis} kNm	τ_e kNm	PF -	η %	M_{cuf} kg	M_{cus} kg	M_{Tot} kg	P_L/V_a kW/m^3	τ_e/V_a kNm/m^3
OS-WF-FSM	16.42	17.70	4.78	3.33	0.87	0.61	1.48	143.48	-	-	4.63	0.67	93.73	51.05	51.05	622.93	56.55	27.28
IS-WF-FSM	64.76	34.44	2.26	1.57	0.29	0.21	0.50	31.57	-	-	1.07	0.51	87.93	31.42	31.42	274.12	75.04	18.50
OS-DC-VRM	11.68	18.10	3.32	2.10	0.89	0.70	1.59	127.10	-	-	4.01	0.81	94.77	48.33	43.82	637.08	41.33	23.62
IS-DC-VRM	36.24	27.85	1.11	1.75	0.46	0.35	0.81	25.10	-	-	0.91	0.14	87.22	19.15	43.38	286.55	63.68	15.72
DS1	11.83	20.94	6.83	4.75	1.16	0.21	1.37	185.38	4.60	1.10	5.70	0.60	93.47	82.47	82.47	891.52	76.30	33.59
DS2	15.25	18.43	4.28	3.85	1.38	0.29	1.67	152.39	4.02	0.90	4.92	0.60	93.96	67.47	87.20	930.28	57.75	28.99
DS3	10.06	17.75	5.61	3.68	1.19	0.35	1.54	158.60	4.02	1.08	5.08	0.66	93.61	79.74	75.24	917.85	63.86	29.96
DS4	18.77	15.26	5.33	4.99	1.32	0.36	1.68	169.03	4.63	0.90	5.53	0.53	93.38	70.20	94.44	903.95	70.61	32.92

N.B. $\Delta\tau_{NL}$ = per unit cogging torque, $\Delta\tau_L$= per unit torque ripple, P_{Fes} = total stator core loss, P_{Fer} = rotor core loss, P_{Fe} = total core loss, length, D_i = stator inner diameter, P_g = generated output power, τ_{eos} = outer stator average torque, τ_{eis} = inner stator average torque, M_{cuf} = total field winding mass, M_{cus} = total phase winding mass, M_{Tot} = total active mass, P_L = total losses, V_a = total active volume

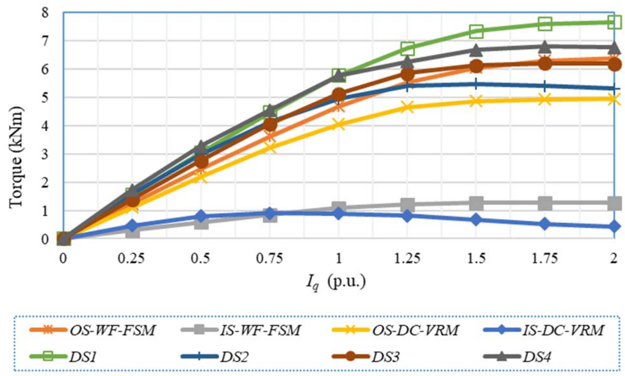

Fig. 11. Overload capability in terms of average torque and at rated I_f.

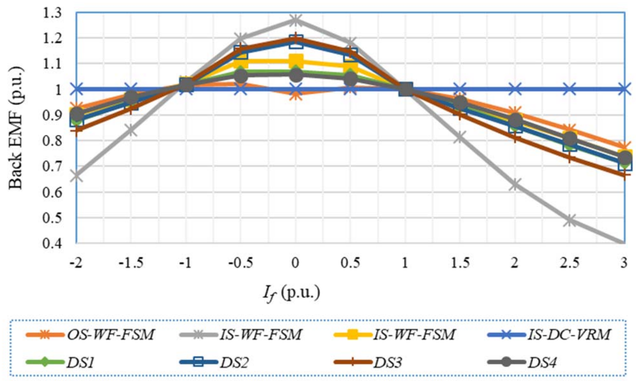

Fig. 12. Field regulation with respect to generated back-EMF at I_q = rated, and 300 r/min.

V. CONCLUSION

In this study, we have shown how the high split ratios of conventional WF-FFMs can be exploited to improve their torque density performance. To this end, four novel DS WF-FFMs, based on the outer and inner stator topologies of the WF-FSM and DC-VRM variants, have been conceived, presented and analysed in 2D FEA magneto-static. As expected, the results indicate performance prominence of the proposed DS machines in terms of torque density, efficiency and torque ripple compared to the generic designs. In one of the proposed DS machines (*DS1*), the torque density improved by as much as 23 % compared to its respective outer single-stator machine, while about 3 % increase in efficiency is obtained compared to the average between the individual single-stator machines. Among other things, this is due to much lower core loss tendencies exhibited in the proposed DS machines. Besides, it is observed that due to higher magnetic flux and torque waveform offset of the respective single-stator machines, the torque ripple as well as cogging torque, can be reduced to as much as 30 %. But with these performance improvements, it is seen that the mass of the DS machines can be increased e.g., to as much as 43 % for *DS1*.

The reported overload capability exceed those of some existing PM-FMMs while being inhibited by high saturation levels. However, it has to be said that all the investigated machines have not been optimised. It is hoped that the analysis presented in this study gives precedence for upgrading the newly formed non-PM DS machines to become industrially competitive high-torque density direct-drive systems. Still promised in the near future, are further analysis, optimisation and experimentation.

VI. REFERENCES

[1] T. Jahns, "Getting rare–earth magnets out of EV traction machines," *IEEE Electrification Magazine*, pp. 6–18, March 2017.

[2] Y. Gao, D. Li, R. Qu, H. Ding and W. Kong, "A Novel Double Stator Flux Modulation Machine With Low-Temperature Superconducting Windings," *IEEE Transactions on Applied Superconductivity*, 28(3), pp. 1-6, April 2018, Art no. 5200406.

[3] S. Jia, R. Qu, J. Li and D. Li, "Principles of Stator DC Winding Excited Vernier Reluctance Machines," *IEEE Transactions on Energy Conversion*, 31(3), pp. 935-946, Sept. 2016.

[4] Z. Chen, H. Wang, Y. Yan, "A doubly salient starter/generator with two-section twisted-rotor structure for potential future aerospace application", *IEEE Trans. Ind. Electron.*, 59(9), pp. 3588-3595, Sep. 2012.

[5] W. Liu, H. Wang, Y. Wang, L. Ren, and L. Xiao, "New approach to suppress torque ripple and improve torque output for wound-excited doubly salient machine," *IECON 2016 - 42nd Annual Conference of the IEEE Industrial Electronics Society*, Florence, pp. 2857-2861, 2016.

[6] F. Khan, E. Sulaiman, and Md Z. Ahmad. "Review of Switched Flux Wound-Field Machines Technology", *IETE Technical Review*, 34(4), 343-352, 2017.

[7] X. Liu and Z.Q. Zhu, "Electromagnetic performance of novel variable flux reluctance machines with DC-Field coil in stator," *IEEE Trans.Magn.*, 49(6), pp. 3020-3028, Jun. 2013.

[8] U. B. Akuru and M. J. Kamper, "Intriguing Behavioural Characteristics of Rare-Earth-Free Flux Switching Wind Generators at Small- and Large-Scale Power Levels," *IEEE Trans. Ind. Appl.*, 54(6), pp. 5772-5782, Nov/Dec 2018.

[9] Z. Zong, L. Quan and Z. Xiang, "Comparison of double-stator flux-switching permanent magnet machine and double-stator permanent magnet synchronous machine for electric vehicle applications," *2014 17th International Conference on Electrical Machines and Systems (ICEMS)*, Hangzhou, 2014, pp. 234-239.

[10] J. Yu and C. Liu, "Design of a Double-Stator Magnetless Vernier Machine for Direct-Drive Robotics," *IEEE Transactions on Magnetics*, vol. 54, no. 11, pp. 1-5, Nov. 2018, Art no. 8105805.

[11] Z. Q. Zhu, Z. Z. Wu and X. Liu, "A Partitioned Stator Variable Flux Reluctance Machine," *IEEE Transactions on Energy Conversion*, vol. 31, no. 1, pp. 78-92, March 2016.
[12] Zi Qiang Zhu, "Overview of novel magnetically geared machines with partitioned stators", *Electric Power Applications IET*, 12(5), pp. 595-604, 2018.
[13] Z. Q. Zhu, Z. Z. Wu, D. J. Evans and W. Q. Chu, "A Wound Field Switched Flux Machine With Field and Armature Windings Separately Wound in Double Stators," *IEEE Transactions on Energy Conversion*, vol. 30, no. 2, pp. 772-783, June 2015.
[14] J. Yu and C. Liu, "DC-Biased Operation of a Double-Stator Hybrid Flux Switching Permanent-Magnet Machine," *IEEE Transactions on Magetics*, vol. 56, no. 2, pp. 1-6, Feb. 2020, Art no. 7505106.
[15] J. T. Chen and Z. Q. Zhu, "Winding Configurations and Optimal Stator and Rotor Pole Combination of Flux-Switching PM Brushless AC Machines," *IEEE Transactions on Energy Conversion*, 25(2), pp. 293-302, June 2010.
[16] X. Liu and Z.Q. Zhu, "Stator/rotor pole combinations and winding configurations of varible flux reluctance machines," *IEEE Trans. Ind. Appl.*, 50(6), pp. 3675-3684, Nov./Dec. 2014.
[17] Liren Huang, Z. Q. Zhu, Jianghua Feng, Shuying Guo, J. X. Shi, Wenqiang Chu, "Analysis of Stator/Rotor Pole Combinations in Variable Flux Reluctance Machines Using Magnetic Gearing Effect", *Industry Applications IEEE Transactions on*, 55(2), pp. 1495-1504, 2019.
[18] D. Li, R. Qu and J. Li, "Topologies and analysis of flux-modulation machines," *2015 IEEE Energy Conversion Congress and Exposition (ECCE)*, Montreal, QC, 2015, pp. 2153-2160.
[19] X. Zhu, C. H. T. Lee, C. C. Chan, L. Xu and W. Zhao, "Overview of Flux-Modulation Machines Based on Flux-Modulation Principle: Topology, Theory and Development Prospects," *IEEE Transactions on Transportation Electrification*, Early Access, 19 Mar 2020.
[20] SEMFEM online resource: www0.sun.ac.za/semfem/index.html
[21] M. Mabhula, U. B. Akuru, and M. J. Kamper "Numerical Estimation of Cross-Coupling Inductance Effects on the Performance of Wound-Field Flux Modulation Machines," INTERMAG AMERICAS, Montreal, Canada, pp. 405, May 4-8, 2020.
[22] T. Fukami, H. Aoki, K. Shima, M. Momiyama and M. Kawamura, "Assessment of Core Losses in a Flux-Modulating Synchronous Machine," *IEEE Transactions on Industry Applications*, 48(2), pp. 603-611, March-April 2012.
[23] M. A. Noroozi, S. Shafiei and J. Milimonfared, "Novel Single Phase E-Shaped Double-Stator Flux Switching Permanent Magnet Generator," *11th Power Electronics, Drive Systems, and Technologies Conference (PEDSTC)*, Tehran, Iran, 2020, pp. 1-5.
[24] J. H. J. Potgieter and M. J. Kamper, "Double PM-rotor, toothed, toroidal-winding wind generator: A comparison with conventional winding direct-drive PM wind generators over a wide power range," *IEEE Transactions on Industry Applications* 52(4), pp. 2881-2891, Jul-Aug., 2016.
[25] L. Shao, W. Hua, J. Soulard, Z. Zhu, Z. Wu and M. Cheng, "Electromagnetic Performance Comparison Between 12-Phase Switched Flux and Surface-Mounted PM Machines for Direct-Drive Wind Power Generation," *IEEE Transactions on Industry Applications*, 56(2), pp. 1408-1422, March-April 2020.

VII. Biographies

Udochukwu B. Akuru (M'13–SM'19) obtained the PhD degree in Electrical Engineering from Stellenbosch University, South Africa in December 2017, and both the MEng and BEng degrees from University of Nigeria, Nsukka, in June 2013 and August 2008, respectively. He is currently a Senior Lecturer at Tshwane University of Technology, South Africa. He held a postdoctoral research fellowship in Stellenbosch University, South Africa, between 2008 and 2020. He is also affiliated to the University of Nigeria, Nsukka, since August 2011.

He is a registered engineer of the Council for the regulation of Engineering in Nigeria (COREN), Senior Member of IEEE, Senior Member of SAIEE, South Africa National Research Foundation (NRF) rated researcher, Member of the Nigeria Young Academy (NYA), and volunteer to various societies, committees and groups such as IEEE IAS EMC and IEEE IES EMTC. His main research interests are in electrical machines design and renewable energy technologies, with competency in finite element analysis and modelling of electrical machines. Dr. Akuru has over fifty peer–reviewed journal and conference papers, and also acts as a reviewer to many IEEE conferences and transactions, among others.

Maarten J. Kamper (SM'08) received the M.Sc (Eng.) degree in 1987 and Ph.D degree in 1996, both from the University of Stellenbosch, Stellenbosch, South Africa. He has been with the academic staff of the Department of Electrical and Electronic Engineering, University of Stellenbosch, since 1989, where he is currently a Professor of electrical machines and drives.

His research interests include computer–aided design and control of reluctance, permanent magnet, and inductance machine drives. Prof. Kamper is a South African National Research Foundation Supported Scientist and a Registered Professional Engineer in South Africa.